APPLICATION OF ULTRASONIC WAVE FIELDS TO MESH FILTRATION OF PARTICLES

D. L. Feke
Department of Chemical Engineering, Case Western Reserve University, Cleveland, Ohio, 44106-7217 USA
dlf4@cwru.edu

Abstract

The separation of micron to millimeter sized solids from their suspending liquid is of fundamental importance in a variety of materials processing applications. In our laboratory, we have developed a unique separation technique in which the application of ultrasonic standing wave fields enables the collection of such solids within meshes having pore size up to 100 times the size of the particles being retained. As a means to understand the fundamental physics of this process, we have developed both microscale and macroscale models of the behavior of suspended particles in our laboratory-scale acoustic devices and have performed experiments to validate these models. The correspondence between observed particle trajectories and pure predictions (from the trajectory analysis model) is excellent. The macroscopic model accurately predicts particle collection dynamics and breakthrough times. These models thus reveal the fundamental physics that underlies the enhancement of mesh filtration by ultrasonic fields.

Introduction

Filtration is the traditional method used for particle-liquid separation. Advanced methods use external fields (such as electrical, magnetic, or centrifugal) to enhance the efficiency of filtration. In our work, we extend this concept to include the use of ultrasonic fields to enhance the efficiency of filtration processes. Our method is believed to have many inherent advantages, such as that it does not rely on a density contrast between the particles and their suspending fluids, any magnetic or electrical susceptibility of the dispersate, and avoids elements that have small (micron-scale) openings that are prone to fouling.

In our method, we typically activate a standing wave field (0.5-1.0 MHz) in a multiwavelength rectangular chamber. The chamber is filled with a very porous mesh having pore openings up to 100 times the diameter of particles to be collected. A suspension of these particles is then pumped through the mesh. When the ultrasonic field is not applied, the suspension flows through the mesh unimpeded. Upon application of the ultrasonic field, up to 90-95 % of the particles can be retained within the mesh. Upon termination of the ultrasonic field, the entrapped particles are then released. Please refer to [1, 2] for additional experimental details.

In addition to the particle retention behavior noted above, our experiments have also shown other interesting phenomena. For example, there appear to be certain preferred positions within the mesh to which particles are guided by the combination of the acoustic and flow fields that are present. This results in the formation of retained clusters of particles that have a dendritic structure. In other cases, we see the formation of particle clusters that are stably retained even though they are not physically in contact with any solid surface within the chamber.

In order to understand all of these behaviors, we recently published [3] a model for the trajectories of individual suspended particles near one element of the collection mesh. This model qualitatively reproduced the various physical phenomena (preferred collection positions that would lead to the formation of dendritic clusters, stable collection points where particle clusters could reside, etc.) that we have observed in our experiments. In addition, this model provided prediction of the capture efficiency of single elements as a function material and acoustic field parameters.

The purpose of this paper is to provide a quantitative verification of the predictions of our single-collector, trajectory analysis model. To do this, we constructed a single-collector experiment that has a geometric configuration that can precisely be simulated by the single-collector model. In this way, observed and predicted motion of particles in the vicinity of this collector could be compared. The agreement between prediction and experiment is quite good.

In addition, we present the results of a second model designed to predict the overall behavior of acoustically aided mesh filtration devices. This model integrates the predictions of the single-collector model to provide predictions of the concentrations of retained particles as a function of position and time within the whole mesh. Predictions of the concentration of unretained particles emerging from the mesh as a function of time can be compared to experimental results. Here too, the ability of the overall process model to predict experimental outcomes is quite good.

The Single-Collector Model

The single-collector trajectory analysis model computes particle trajectories on the basis of the hydrodynamic and acoustic forces acting within the vicinity of a single cylinder. Figure 1 shows a schematic of the simulation geometry employed. Both the flow and the acoustic field are presumed to be oriented perpendicular to the axis of the cylinder, but the relative angle between the acoustic and flow

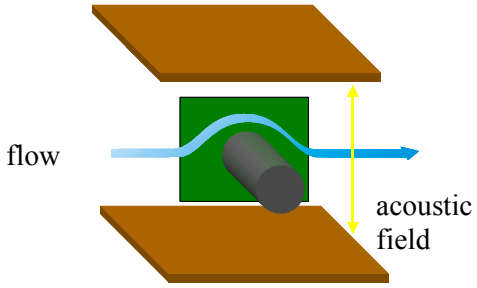

Figure 1: Schematic of simulation geometry for the single-collector model.

field is arbitrary. In addition, the position of the cylinder can be varied with respect to the acoustic nodes.

Particle trajectories are sensitive to three relevant dimensionless groups: the Reynolds number (*Re*) determines the fluid streamlines in the vicinity of the cylinder; the Gorkov number (*Gk*) represents the ratio of the acoustic forces acting on the suspended particles relative to the hydrodynamic drag forces; and the Archimedes number (*Ar*) gauges the effect of gravity on the motion of particles near the cylinder. Please see [3] for additional details.

Figure 2 shows typical simulation results. In this particular case, the axis of the cylinder is located one-tenth of an acoustic wavelength from the nodal plane of the incident field, $Re = 0.1$, $Gk = 0.42$, and $Ar = 0$. The field of arrows depicts the direction that a particle located at that position would travel in response to the combination of acoustic and drag forces. The solid lines represent the trajectories of particles launched from the left toward the cylinder (the circle at the center). Note that there exist preferred angular positions on the cylinder at which trajectories bring particles to its surface. Note also that the cylinder intercepts particles from a region in space larger than

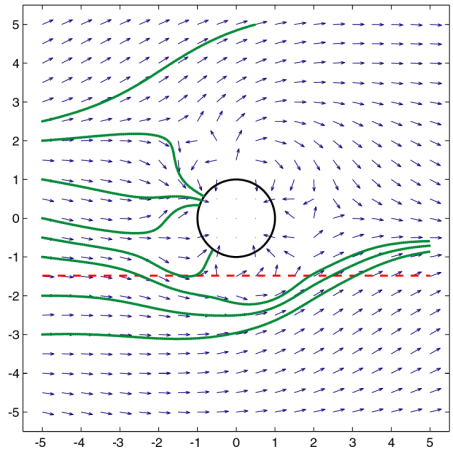

Figure 2: Plots of particle trajectories predicted by the single-collector model for the case of $Re = 0.1$, $Gk = 0.42$, and $Ar = 0$

the size of the cylinder itself. Computation of this "upstream interception area" provides a qualitative basis for the particle collection phenomena observed in our laboratory experiments.

Single-Collector Experiments

In order to validate in detail the predictions of the single-collector model, an experimental chamber was constructed to allow direct visualization of the motion of particles near a cylindrical collector. A single cylindrical collector (0.6 mm diameter stainless steel wire) was fixed within a rectangular acoustic chamber such that its axis is perpendicular to both the acoustic and flow fields. A dilute suspension of polystyrene particles (54μm diameter) was passed through the chamber. The sidewalls of the chamber and the reflector wall were constructed of transparent materials. External optics allowed a thin laser sheet (532 nm) to illuminate a portion of the chamber. A digital video camera (30 frames/s, 1024× 1024 pixels, 10 bit grayscale) was positioned outside the sidewall along the axis of the cylindrical wire.

Figure 3 shows a typical still image obtained from this experimental chamber. The large circle at the center is the cross-section of the cylindrical wire. The smaller points are particles present within the illuminated laser sheet. Fluid flow passes from top to bottom of this image. Typically, sequences of images covering several seconds of operation are recorded. Following conditioning of such images, particle-tracking software is then used to obtain information on the position of individual particles as a function of time.

The trajectories of two specific particles are also superimposed within Figure 3. Note that although the particles originate at different locations within the chamber, their trajectories eventually converge and

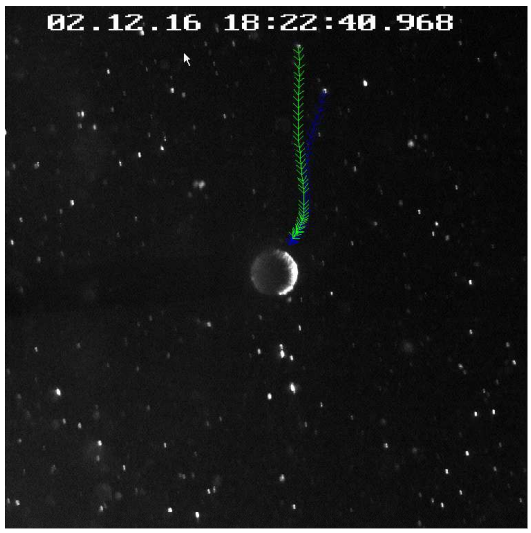

Figure 3: Images of particles and particle trajectories obtained from the experimental chamber.

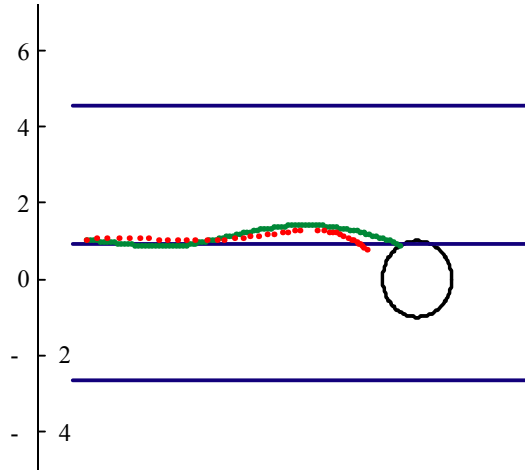

Figure 4: Comparison of observed (red) and predicted (green) trajectories for the case of Re = 0.1 and Gk = 0.81.

both particles collide with the cylinder at the same angular position as was suggested by the single-collector trajectory model.

Figure 4 shows a sample comparison of a particle trajectory viewed in a single-collector experiment (red) and the trajectory predicted by the single-collector model (green). Note that the simulation result is based on the use of the various material, geometric, and operating parameters present within the experiment. The predicted trajectories include the effects of the acoustic field scattered off of the cylindrical collector.

Calculation of the predicted trajectories requires knowledge of the acoustic energy density within the liquid medium. However, since we do not have a direct means of measuring this parameter, we resort to inferring the value of the acoustic energy density from information on the electrical signal powering the piezoelectric transducer. For this purpose, we have relied on a multi-layer transmission model of Rusinko [4]. Based on this approach, the value of the Gorkov number for the particular experiment shown in Figure 4 is predicted to be Gk = 0.81.

The match between the observed and predicted trajectories is excellent for the particular case shown in Figure 4. Comparisons of observed and predicted trajectories for particles that do not pass so close to the cylinder show less agreement, however. Improvements in the match can be obtained by performing trajectory calculations using different values of Gk. This is justified for several reasons. First, the precision of the multilayer resonance model in predicting the value of acoustic energy density from the electrical signal powering the piezoelectric transducer is not known. Secondly, it is likely that strength of the acoustic field will vary within the chamber due to attenuation effects. Lastly, it is reasonable to expect that the acoustic energy density within the chamber may vary with position along a specific trajectory. However, the single-collector trajectory model assumes a single value of Gk throughout the chamber.

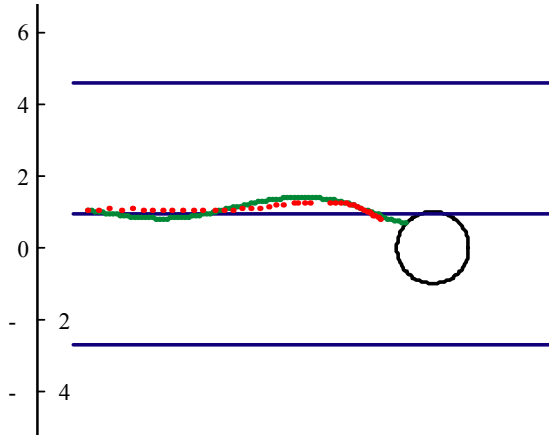

Figure 5: Comparison of observed and predicted trajectories for the case of Gk = 1.10

Figure 5 shows the same experimental trajectory as presented in Figure 4, but a predicted trajectory using Gk = 1.10. A numerical metric was developed to quantify the goodness of fit between the observed and predicted trajectories, and this metric was optimized at this particular value of Gk. Note the excellent match.

Figure 6 shows the trajectory of another particle from the same experiment (computed Gk = 0.81) but with the trajectory computed using Gk = 0.29. Note that there is virtually no discrepancy between the two.

In order to explain the result that different values of Gk were used for the two particle trajectories, we note that the orientation of the experimental chamber is such that the piezoelectric transducer is located off the bottom of the images in Figures 4-6. Thus, one may expect that the intensity of the acoustic field would diminish in the upward vertical direction of these graphs. The result that the optimum Gk was found to be lower for particle trajectories that are located further from the transducer in comparison to trajectories that pass closer to the transducer is consistent with this notion. This indicates that attenuation in the acoustic energy density apparently

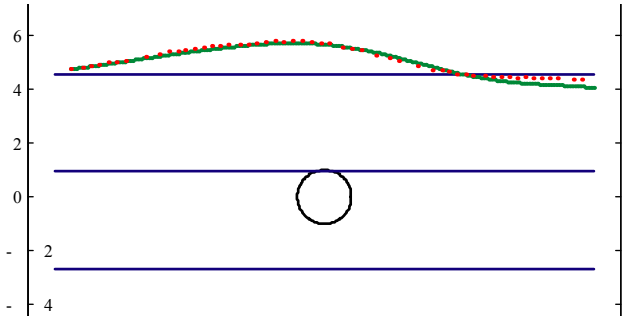

Figure 6: Comparison of an experimental trajectory to one predicted for the case of Gk = 0.29

increases with distance relative to the transducer.

Macroscopic Process Model

An additional modeling interest is to predict the overall retention behavior of acoustically driven porous meshes as a function of system and operating parameters. The single-collector model can be used to make predictions on the numbers of particles that are captured by an individual element within the porous mesh. Our goal is to build on that information and construct an overall process filtration model.

Using $C(x, \tau)$ to denote the concentration of particles free to move within the liquid as a function of position within the mesh and operating time, and $N(x, \tau)$ to denote the concentration of entrapped particles, the continuity equation gives

$$\frac{\partial N}{\partial \tau} + v_o \frac{\partial C}{\partial x} = 0 \qquad (1)$$

where v_0 is the superficial velocity of the liquid moving through the mesh. The local rate of conversion of free particles into entrapped particles is given by a kinetic equation of the form

$$\partial N/\partial \tau = f(C, N) \qquad (2)$$

By averaging the interception area results from the single-collector trajectory model over the whole set of possible relative configurations of cylinder, flow, and acoustic field, this kinetic expression can be determined. This approach is analogous to that commonly used to extrapolate single-collector modeling results to predict collection in random meshes [5].

Once the relationship expressed in (2) is known, the continuity equation (1) can be solved. Figure 7 shows typical results. Shown are experimental data [1] for the capture of 27 μm polystyrene particles in a 1.0 wt % aqueous suspension flowing through a 20 ppi (pores per inch) mesh at 30cm^3/min. Prior to zero

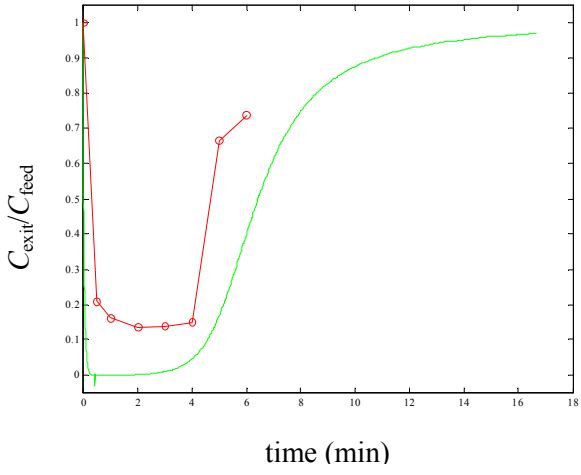

Figure 7: Comparison of the prediction of the macroscopic model (continuous curve) to experimental results reported in [1] (line with data markers).

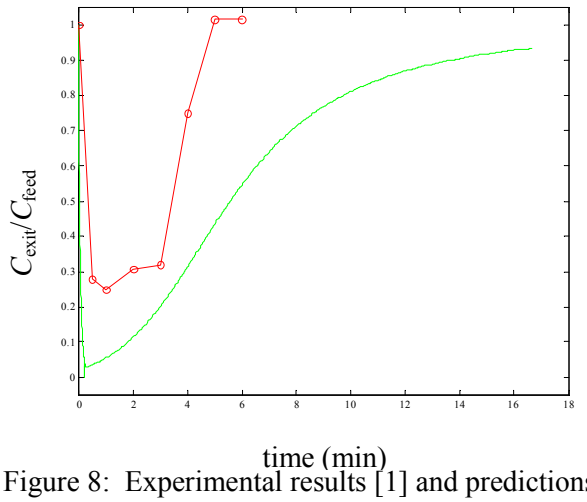

Figure 8: Experimental results [1] and predictions of the macroscopic model for the case of doubled flow, but halved concentration compared to the results shown in Figure 7.

time there is no acoustic field applied, and the suspension flows through the mesh unimpeded. At zero time, the acoustic field is energized and the concentration of particles in the liquid exiting the chamber is monitored as a function of time. Figure 7 shows that the exit concentration of particles quickly drops to about 15% of its inlet value and remains at that value for about 4 min total. At that time, the porous mesh has reached a saturation limit, and higher concentrations of particles are observed in the effluent liquid. The breakthrough time is that for which the effluent particle concentration begins to rise rapidly.

The continuous line in Figure 7 represents the predictions of the macroscopic model. One again, it should be emphasized that this is a complete prediction, based on the results of the single-collector trajectory analysis. The shape of the macroscopic model prediction matches well to the experimental results. In addition, the breakthrough time predicted by the model duplicates the experimental results.

Figure 8 shows another comparison between the macroscopic model prediction and experimental data for the case of the flow rate doubled (to 60 cm^3/s) and the particle concentration halved (to 0.5 wt% solids). At the outset, one may expect to see the breakthrough time in this case match that shown in Figure 7. However, the data do not show this result, which stems from the fact that the value of Gk in the two sets of data are different. Nevertheless, the predictions of the macroscopic model again mimic the overall filtration performance for this case. This result demonstrates the sensitivity of both the single-collector trajectory analysis model and the macroscopic performance model to the details of the acoustic field acting within the experiments.

Table 1 presents a direct comparison of the predicted and experimental breakthrough times for three sets of experiments. Overall, the macroscopic model

Table 1: Comparison of experimental and predicted breakthrough times.

Flow rate (cm^3/min)	Solids Loading (wt%)	Breakthrough time (min)	
		Experiment	Model
30	0.5	10	9
60	0.5	3	1.5
30	1.0	4	4.5

performs well. It is reasonable to expect that by carefully adjusting model parameters, even better correspondence could be obtained. Nevertheless, the macroscopic model results do show predictions that scale correctly with both fluid flow rates and solids loading in the feed.

Conclusions

1. The single-collector trajectory model predicts the various phenomena observed in mesh filtration experiments. These include the formation of entrapped particles having a dendritic structure, and favored positions for the collection of particles on elements of the mesh.
2. The results from the single-collector experiments quantitatively verified the accuracy of the single-collector trajectory analysis. Good correspondence between observed and predicted trajectories was seen, even for the case of no adjustments in model parameters.
3. Optimization of the fit between observed and predicted trajectories yields information on the spatial variation of the acoustic energy density within the experimental chamber. Results suggest that attenuation of the acoustic field scales with the distance from the source transducer.
4. Results from the single-collector modeling efforts could be used as part of a macroscopic model for the overall performance of the mesh filtration devices.
5. Pure predictions from the macroscopic model (i.e., without fitting any model parameters) resulted in predictions that matched well to the performance dynamics of ultrasonically driven mesh filtration.
6. The predictions of the macroscopic model were seen to scale appropriately with liquid flow rate and particle concentration within the feed.

Acknowledgment

This work was supported by a grant from the National Aeronautics and Space Administration (NRA-97-HEDS-02-100). The contributions of Michael Grossner and Joanne Belovich to this work are gratefully acknowledged.

References

[1] S. Gupta and D.L. Feke, "Filtration of particulate suspensions in an acoustically driven porous media," A.I.Ch.E. Journal, vol. 44, pp. 1005-1014 (1998).

[2] S. Gupta and D.L. Feke, "Acoustically driven collection of suspended particles within porous media," Ultrasonics, vol. 35, pp. 131-139 (1997).

[3] M.T. Grossner, A.E. Penrod, J. M. Belovich, and D.L. Feke, "Single-fiber model of particle retention in an acoutsically driven porous mesh," Ultrasonics, vol. 41, pp. 65-74, (2003).

[4] D.M. Rusiko, "Design and Optimization of an Ultrasonic Standing Wave Chamber," M.S. Thesis, Case Western Reserve University (2001).

[5] M.T. Grossner, "Study of Particle Retention in Ultrasonically Enhanced Separation Processes," Ph.D. Dissertation, Case Western Reserve University (2003).